*Abstract for the 29th Intl Workshop on Water Waves and Floating Bodies, Osaka (Japan), March 30 April 02, 2014*

# Wave scattering by dual Surface-Piercing Porous and Flexible Barriers

**Sourav Mandal*, Harekrushna Behera and Trilochan Sahoo**

Department of Ocean Engineering and Naval Architecture
Indian Institute of Technology, Kharagpur -721 302, India
E-mail: *souravmath88@gmail.com*

## Highlights

- Scattering of obliquely incident surface waves by dual surface-piercing permeable flexible barriers in a two-layer fluid having free surface and an interface are studied.
- The mathematical problem is handled for solution using a generalized orthogonal relation suitable for two-layer fluid along with the least square approximation method.
- Effect of oblique angle and barrier spacing are analyzed numerically to study the efficiency of the flexible porous barriers in creating a tranquility zone.
- The proposed dual barrier system is expected to be an efficient method for protecting various coastal infrastructure from wave attack.

## 1. Introduction

In recent decades, emphasis is given for the dynamic analysis of wave interaction with flexible breakwaters to develop quickly deployable, reusable and low cost wave attenuation and protection systems. Ren and Wang [1] studied the wave scattering by a flexible porous breakwater which is anchored to the sea bed. Recently, Behera et al. [2] studied oblique wave trapping by porous and flexible structures in a two-layer fluid by analyzing the effect of critical angle of incidence on the oblique wave trapping by barriers. In the present study, oblique wave scattering by surface-piercing dual flexible porous barriers are analyzed in finite water depth in a two-layer fluid domain having a free surface and an interface.

## 2. Mathematical formulation

In the present study, the problems are considered in the three dimensional Cartesian coordinate system in water of finite depth $H$, with $z$- axis being vertically upwards and the fluid domain being separated by an undisturbed interface located at $z = -h$ and the upper fluid is having an undisturbed free surface located at $z = 0$ as in Fig. 1. The notations $L_b$ and $L_g$ represent the submerged portion of the barrier and the gap respectively and are given as $L_b = (-a \leq z \leq 0)$ and $L_g = (-H \leq z \leq -a)$. It is assumed that barriers are placed at $x = \pm L$. The fluid domain is divided into three regions with Region 1: $(-\infty < x < -L)$, Region 2: $(-L < x < L)$ and Region 3: $(L < x < \infty)$ with $-H < z < 0$. It is assumed that the incident wave in surface and interface modes are propagating making an oblique angle $\theta$ with the $x-$axis. The fluid is assumed to be inviscid and incompressible and the flow is assumed to be irrotational and simple harmonic in time and angular frequency $\omega$ which ensures the existence of the velocity potentials $\Phi_j$ such that $\Phi_j(x, y, z, t) = \mathrm{Re}\{\phi_j(x, z)\mathrm{e}^{\mathrm{i}(k_y y - \omega t)}\}$ with $k_y = k_j \sin\theta$, $k_j$ for $j = I, II$ refers to the waves in surface and internal modes respectively. The velocity potential $\Phi_j$ satisfies the reduced wave equation

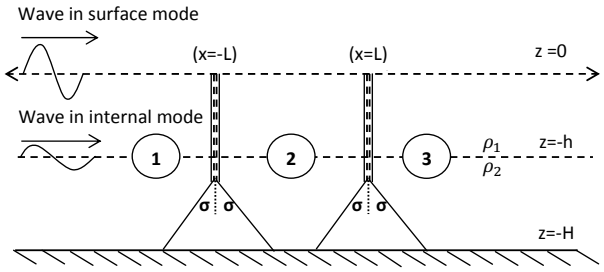


Fig. 1. Schematic diagram for wave scattering by dual surface-piercing porous and flexible barriers

$$(\partial_x^2 + \partial_z^2 - k_y^2)\phi_j = 0, \tag{1}$$

along with the linearized free surface boundary condition is given by

$$\partial_z \phi_j - K\phi_j = 0, \quad x \in I_j \quad (j = 1, 2, 3) \quad \text{on } z = 0, \tag{2}$$

where $K = \omega^2/g$, $g$ is the gravitational constant and $I_1 = (-\infty, -L), I_2 = (-L, L)$ and $I_3 = (L, \infty)$ with subscript $j$ in the velocity potential referring to the $j$th fluid domain. On the other hand, the linearized boundary conditions at the interface are given by

$$\partial_z\phi_j\Big|_{z=-h_-} = \partial_z\phi_j\Big|_{z=-h_+} \quad \text{and} \quad \Big(\partial_z\phi_j - K\phi_j\Big)\Big|_{z=-h_-} = s\Big(\partial_z\phi_j - K\phi_j\Big)\Big|_{z=-h_+}, \quad \text{for } j = 1, 2, 3, \tag{3}$$

where $s = \rho_1/\rho_2$ with $0 < s < 1$. The boundary condition at the rigid bottom bed is given by given

$$\partial_z\phi_j = 0, \quad (j = 1, 2, 3) \quad \text{on } z = -H. \tag{4}$$

The scattered potentials in Regions 1 and 3 satisfy the far field boundary conditions

$$\phi_1 \sim \sum_{n=I}^{II} \Big(I_n \mathrm{e}^{\mathrm{i}q_n(x+L)} + R_n \mathrm{e}^{-\mathrm{i}q_n(x+L)}\Big)\psi_n(z), \quad \text{as} \quad x \to -\infty, \tag{5}$$

$$\phi_3 \sim \sum_{n=I}^{II} T_n \mathrm{e}^{\mathrm{i}q_n(x-L)}\psi_n(z), \quad \text{as} \quad x \to \infty, \tag{6}$$

where $I_n$, $R_n$ and $T_n$ for $n = I, II$ are constants associated with the incident, reflected and transmitted wave amplitudes in SM and IM respectively with $q_n = \sqrt{k_n^2 - k_y^2}$. It is assumed that $I_n$s are assumed to be known, $R_n$ and $T_n$ are unknowns to be be determined. The wave numbers $k_I$ and $k_{II}$ correspond to the waves in SM (surface mode) and IM (internal mode) respectively. In Eqs.(5)-(6), $\psi_n(z)$s are the vertical eigenfunctions associated with the plane gravity waves in two-layer fluid to be defined in the forthcoming Section. The continuity of pressure and normal velocity near $x = \pm L$ $(j = 1, 2)$ is given by

$$\phi_j = \phi_{j+1}, \quad z \in L_g, \quad \text{and} \quad \phi_{jx} = \phi_{(j+1)x}, \quad z \in L_g \cup L_b. \tag{7}$$

Assuming that the transverse deflection of the flexible porous barrier is small compared to the water depth and is of the form $\zeta(y, z, t) = \mathrm{Re}\{\xi(z)\mathrm{e}^{\mathrm{i}(k_y y - \omega t)}\}$ with $\xi(z)$ being the complex deflection amplitude, $k_y$ and $\omega$ being the same as defined earlier. Using Darcy law for flow past a porous structure, the body boundary condition on the $j$th porous and flexible barrier is given by

$$\partial_x\phi_j = \mathrm{i}k_I G(\phi_j - \phi_{j+1}) - \mathrm{i}\omega\xi_j, \quad \text{at} \quad x = \pm L \quad \text{for} \quad j = 1, 2 \quad \text{and} \quad z \in L_b, \tag{8}$$

with $G$ being the complex porous-effect parameter as in Mandal et al. [3]. The barriers are assumed as thin elastic plates of uniform mass and subject to uniform rigidity and the barrier is idealized as a one-dimensional beam. Thus, the equation of motion for $j$th $(j = 1, 2)$ flexible barrier acted upon by fluid pressure is given by [see 2]

$$\gamma\big(D^2 - k_y^2\big)^2\xi_j + (\beta/H^2)\big(D^2 - k_y^2\big)\xi_j - \alpha\xi_j = \chi(\phi_j - \phi_{j+1}), \quad z \in L_b, \tag{9}$$

where $D = d/dz$ and $\gamma = EI/(\rho_2 g H^4)$ with $EI$ being the uniform flexural rigidity of the barrier, $\beta = -Q/(\rho_2 g H^2)$ with $Q$ being the constant axial force acting on the barrier and $\alpha = (m_s\omega^2)/(\rho_2 g H^4)$ with $m_s = \rho_s d$ the uniform mass per unit length, $\rho_s$ the density of the barrier and $\chi = (\mathrm{i}\omega\rho)/(\rho_2 g H^4)$. The flexible barriers are assumed to be fixed at the free surface and moored at the submerged end as in Fig. 1. Thus, near the moored end bending moment vanishes whilst at the fixed end of the barrier, vanishing of barrier deflection and slope of the barrier deflection yield

$$\big(D^2 - \nu k_y^2\big)\xi_j(-a) = 0, \quad \text{and} \quad \xi_j(0) = 0,\ \xi_j'(0) = 0, \tag{10}$$

with $\nu$ being the Poisson ratio. The boundary condition at the moored tips relates to the horizontal components of the dynamic mooring line tensions and the restoring forces due to the axial load to the shearing forces there and is given by [see 1]

$$\big[EI\big\{D^2 - (2 - \nu)k_y^2\big\}D - QD\big]\xi_j(-a) = 2\pounds \sin^2\sigma\xi_j(-a), \tag{11}$$

with $\pounds$ = mooring line stiffness and $\sigma$ = the mooring line angel in the static position as defined in Fig. 3. Assuming the barriers are interface piercing in nature, the continuity of barrier deflection, slope of deflection, bending moment and the shear force acting on the barrier near the interface yield

$$\xi_j(z),\ \xi_j'(z),\ \big(D^2 - \nu k_y^2\big)\xi_j(z), \quad \text{and} \quad \big[EI\big\{D^2 - (2 - \nu)k_y^2\big\}D - QD\big]\xi_j(z) \quad \text{are continuous at } z = -h. \tag{12}$$

However, the continuity conditions in Eq. (12) will not be required for interface non-piercing barriers.

## 3. Method of solution

The spatial velocity potentials $\phi_j$ in $j$th Region for $j = 1, 2, 3$ satisfying Eq.(1) along with the boundary conditions in Eqs.(2)-(4) and radiation boundary conditions as in Eq.(5)-(6) are expressed as

$$\phi_1 = \sum_{n=I}^{II} I_n \mathrm{e}^{\mathrm{i}q_n(x+L)}\psi_n(z) + \sum_{n=I,II,1}^{\infty} R_n \mathrm{e}^{-\mathrm{i}q_n(x+L)}\psi_n(z), \quad x < -L, \tag{13}$$

$$\phi_2 = \sum_{n=I,II,1}^{\infty} \Big(A_n F_{a_n} \cos q_n x + B_n F_{b_n} \sin q_n x\Big)\psi_n(z), \quad -L < x < L, \tag{14}$$

$$\phi_3 = \sum_{n=I,II,1}^{\infty} T_n \mathrm{e}^{\mathrm{i}q_n(x-L)}\psi_n(z), \quad x > L, \tag{15}$$

with

$$F_{a_n} = \begin{cases} 1, & \text{for} \quad n = I, II, \\ \sec q_n L, & \text{for} \quad n = 1, 2, ..., \end{cases} \quad \text{and} \quad F_{b_n} = \begin{cases} 1, & \text{for} \quad n = I, II, \\ \operatorname{cosec} q_n L, & \text{for} \quad n = 1, 2, .... \end{cases}$$

The eigenfunctions $\psi_n(k_n, z)$ for $n = I, II, 1, 2, ...$ associated with Eq.(13)-(15) are given by

$$\psi_n(z) = \begin{cases} \dfrac{\sinh k_n(H-h)\{k_n \cosh k_n z + K \sinh k_n z\}}{K \cosh k_n h - k_n \sinh k_n h}, & -h < z < 0, \\ \cosh k_n(z+H), & -H < z < -h, \end{cases} \tag{16}$$

and $k_n$s in $k$ satisfies the dispersion relation

$$\mathcal{G}(k) \equiv K^2\{s + \coth kh \coth k(H-h)\} - kK\{\coth kh + \coth k(H-h)\} + k^2(1-s) = 0. \tag{17}$$

It is assumed that the dispersion relation in Eq.(17) has two real positive roots $k = k_I, k_{II}$, infinitely many imaginary roots of the form $k = ik_n$ for $n = 1, 2, ...$ with $k_n$ being real and positive. The complex coefficients $R_n$ and $T_n$ for $n = I, II, 1, 2, 3...$ are unknown constants to be determined. The eigenfunctions $\psi_n(z)$s in Eq. (16) are orthogonal with respect to the inner product defined by [see 2]

$$\langle \psi_m(z), \psi_n(z) \rangle = \rho_2 \int_{-H}^{-h} \psi_m(z)\psi_n(z)dz + \rho_1 \int_{-h}^{0} \psi_m(z)\psi_n(z)dz = \frac{\mathcal{G}'(k_n)\sinh^2 k_n(H-h)}{2K(k_n - K\coth k_n h)}\delta_{mn}, \tag{18}$$

with $\delta_{mn}$ being the Kroneckar delta and $\mathcal{G}(k_n)$ being the same as in Eq.(17). Using Eqs. (13)-(15) in the continuity of velocity conditions at $x = \pm L$ as in Eq. (7) and orthogonal properties of $\psi_n(z)$ as in Eq. (17) yields

$$R_n + T_n - I_n = 2\mathrm{i}A_n F_{a_n} \sin q_n L, \quad \text{and} \quad R_n - T_n - I_n = 2\mathrm{i}B_n F_{b_n} \cos q_n L, \quad n = I, II, \tag{19}$$

$$R_n + T_n = 2\mathrm{i}A_n F_{a_n} \sin q_n L, \quad \text{and} \quad R_n - T_n = 2\mathrm{i}B_n F_{b_n} \cos q_n L, \quad n = 1, 2, ..., \tag{20}$$

Using Eqs. (13)-(15) and the conditions in Eqs. (7)-(8), suitable application the least square approximation method yields a system of equations for the determination of the unknown coefficients in the velocity potentials. Additional edge conditions as in Eqs. (10)-(11) along with the the continuity conditions in Eqs. (12) are incorporated into the system of equations for uniqueness of the solution.

## 4. Numerical results and discussion

A MATLAB program is developed to investigate the effects of the following wave and structural parameters on the reflection, transmission coefficients. In the present study, depth ratio $h/H = 0.5$, $G = 1 + 0.5\mathrm{i}$, time period $T = 8$ sec, acceleration due to gravity $g = 9.81$ m/sec$^2$, density ratio $s = 0.75$, Poisson ratio $\nu = 0.3$, and oblique angle of incidence $\theta = 30^o$, mooring angel $\sigma = 45^o$, mooring line stiffness $\pounds = 2000$ N/m, non-dimensional flexural rigidity $\gamma = EI/\rho_2 g H^4 = 0.1$, uniform force $\beta = Q/\rho_2 g H^2 = 0.1$ and barrier mass $\alpha = m_s/\rho_2 H = 0.1$ are kept fixed unless it is mentioned. The reflection and transmission coefficients in surface and internal modes are computed using the formulae

$$K_{rI} = \left|\frac{R_I}{I_I}\right|, \quad K_{tI} = \left|\frac{T_I}{I_I}\right|, \quad K_{rII} = \left|\frac{R_{II}}{I_{II}}\right| \quad \text{and} \quad K_{tII} = \left|\frac{T_{II}}{I_{II}}\right|. \tag{21}$$

From Figs. 2(a) and (b), it is observed that wave reflection increases due to a decrease in barrier length for waves in SM and IM. However, in the case of interface-piercing barrier, higher wave reflection occurs in internal mode than surface

mode with an increase in barrier length. Both in surface mode and internal mode, minimum in wave reflection are referred as wave trapping in the confined zone between the dual barriers.

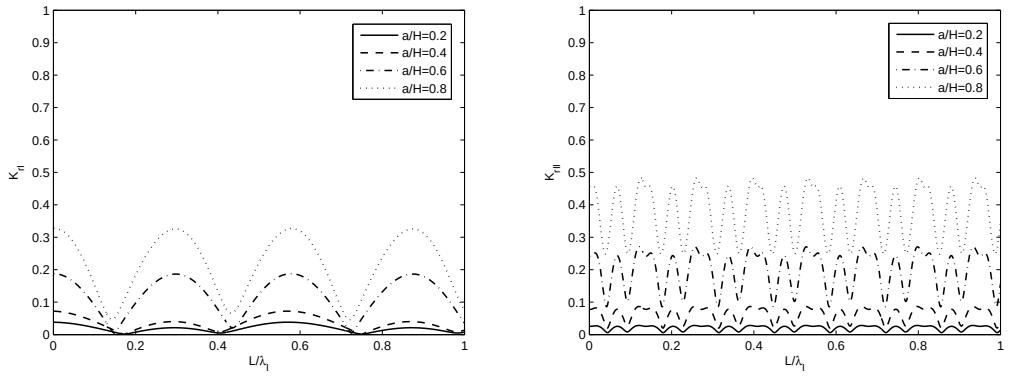


(a) (b)

Fig. 2. Variation of reflection coefficients versus $L/\lambda_I$ in (a) SM and (b) IM for different values of $a/H$ with $G = 1+0.5\mathrm{i}$.

From Figs. 3(a) and (b), it is observed that there is a decrease in the number of optimum values in the refection coefficients in surface mode and vise versa in internal mode within the the same range of $L/\lambda_I$. This may be due to the change in the wavelength of waves in surface and internal modes in the presence of the porous structure and change in angle of incidence. Further, due to dissipation of more wave energy, the reflection coefficient decreases with an increase in the absolute value of the porous-effect parameter $G$.

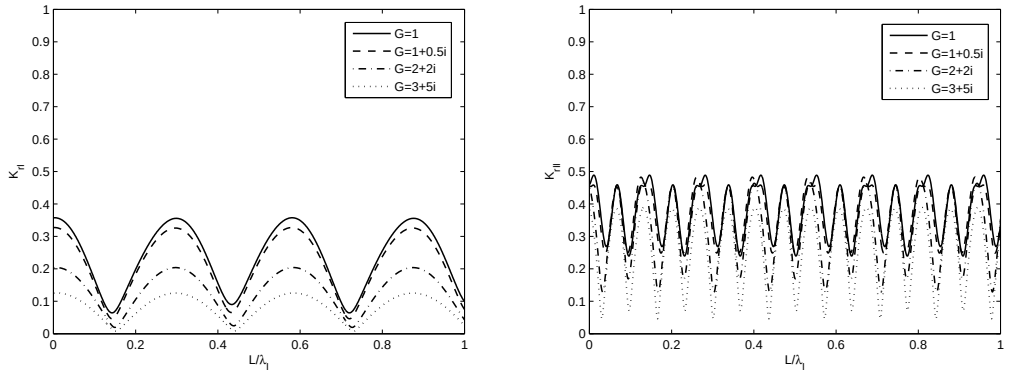


(a) (b)

Fig. 3. Variation of reflection coefficients versus $L/\lambda_I$ in (a) SM and (b) IM for different values of $G$ with $a = 0.8H$.

Computational results on the effect of oblique angle will be presented in the workshop.


## Acknowledgement

SM gratefully acknowledges the financial support received from CSIR, New Delhi to pursue this research work.


# References


[1] Ren, X., and Wang, K. H. "Mooring lines connected to floating porous breakwaters," International Journal of Engineering Science, **32(10)**, 1511-1530 (1994).

[2] Behera, H., Mandal, S., and Sahoo, T. "Oblique wave trapping by porous and flexible structures in a two-layer fluid," Physics of Fluids, **25**, 112110 (2013).

[3] Mandal, S., Datta, N., and Sahoo, T. "Hydroelastic analysis of surface wave interaction with concentric porous and flexible cylinder systems," Journal of Fluids and Structures, **42**, 437-455 (2013).